Supporting Information for

Influence of pH on the Formation of Sulfate and Hydroxyl Radicals in the UV/Peroxymonosulfate System

Ying-Hong Guan [†], *Jun Ma*[*, †, ‡] *Xu-Chun Li*[†], *Jing-Yun Fang*[†], *and Li-Wei Chen*[†]

[†] State Key Laboratory of Urban Water Resource and Environment, Harbin Institute of Technology, Harbin, China, [‡] National Engineering Research Center of Urban Water Resources, Harbin Institute of Technology, China

Corresponding author: Professor Dr Jun Ma

Tel: 86-451-86283010; fax: 86-451-86282292; e-mail: majun@hit.edu.cn. .

Submitted to

Environmental Science & Technology

Prepared on January 3, 2011

Number of pages (including this page): 16

Number of figures: 11

Text S1. Experimental procedure. The UV lamp was turned on for at least 30 minutes before experiments to obtain constant incident intensity. The reaction solution was prepared by adding the desired amount of BA, PMS, and buffer to 1.2 L deionized water and was stirred continuously using a magnetic stirrer for about 30 seconds before the UV lamp was put into the reactor. The error brought in by the delay of mixture could be ignored, because BA was not degraded by PMS alone. TBA was used as the scavenger to capture $HO^{\bullet}$ and methanol was used as the scavenger to capture both $HO^{\bullet}$ and $SO_4^{\bullet-}$ (rate constants can be seen in Table 1). The influences of phosphate/tetraborate buffer on BA degradation were considered. It was shown in Fig S1a and S1b that the phosphate buffer did not interfere with the degradation efficiency of BA even at the concentration of 5 mM at pH 7 (in the forms of $H_2PO_4^-$ and HPO_4^{2-}) and at pH 12 (in the forms of HPO_4^{2-} and PO_4^{3-}). It was also found that the tetraborate buffer did not influence the degradation efficiency of BA at the buffer concentration as high as 5 mM. Hence, the influence of the phosphate/tetraborate buffer on BA degradation at the buffer concentration of 2 mM used in the present study could be neglected. The mixture of sodium nitrite (2 mM) and PMS (100 μM) did not induce the degradation of BA. The difference between the concentrations of BA in the samples quenched by sodium nitrite and that measured immediately without quenching was little (< 3%, results not shown). Hence, sodium nitrite was selected as the quenching reagent.

Text S2. ***EPR measurements.*** 5, 5-dimethyl-1-pyrrolidine N-oxide (DMPO) was used as a spin-trapping agent. The mixture of DMPO and sample was irradiated by UV

lamp for 30s and then sampled by a capillary tube, which was inserted into the EPR cavity. EPR experiments were performed on a Bruker A200 spectrometer. The condition was: a center field of 353.5 mT, a sweep width of 7 mT, a sweep time of 81.92 s, a modulation frequency of 100 kHz, a modulation amplitude of 0.05 mT, a microwave frequency of 9.85 GHz, and a microwave power of 6.1 mW.

Text S3. The kinetic expressions of $SO_4^{\bullet-}$ and $HO^{\bullet}$ in the UV/PMS system could be expressed as eqs S1 and S2 based on the estimation of k_{10a}/ k_{10b} to be 5 at 20°C,[1] since the consumption rate of $SO_4^{\bullet-}$ by PMS and the consumption rate of $HO^{\bullet}$ by SO_4^{2-} were negligible compared with that by BA. The kinetic expression of peroxomonosulfate radical ($SO_5^{\bullet-}$) could be expressed as eq S3. Based on the pseudo-steady state assumption and eqs S4 and S5, the relative quasi-stationary concentration of $SO_4^{\bullet-}$ (*RQSC*) could be derived as eq S6.

$$\frac{dc_{SO_4^{\bullet-}}}{dt} = \phi I_0 b \frac{\varepsilon_{HSO_5^-}[HSO_5^-] + \varepsilon_{SO_5^{2-}}[SO_5^{2-}]}{A□V}(1-10^{-A}) + \frac{10}{6}k_{10}[SO_5^{\bullet-}]^2 - k_{12}[SO_4^{\bullet-}]c_{BA} - k_{17}[SO_4^{\bullet-}]c_{TBA} - k_5[SO_4^{\bullet-}]c_{HO^-} \quad \text{(S1)}$$

$$\frac{dc_{HO^{\bullet}}}{dt} = \phi I_0 b \frac{\varepsilon_{HSO_5^-}[HSO_5^-] + \varepsilon_{SO_5^{2-}}[SO_5^{2-}]}{A□V}(1-10^{-A}) + k_5[SO_4^{\bullet-}]c_{HO^-} - k_{11}[HO^{\bullet}]c_{BA} - k_{16}[HO^{\bullet}]c_{TBA} - k_2[HO^{\bullet}][HSO_5^-] - k_3[HO^{\bullet}][SO_5^{2-}] \quad \text{(S2)}$$

$$\frac{dc_{SO_5^{\bullet-}}}{dt} = k_2[HO^{\bullet}][HSO_5^-] + k_3[HO^{\bullet}][SO_5^{2-}] - 2k_{10}[SO_5^{\bullet-}]^2 \quad \text{(S3)}$$

$$Ka_1 = \frac{[H^+][SO_5^{2-}]}{[HSO_5^-]} \quad \text{(S4)}$$

$$c_{PMS} = [HSO_5^-] + [SO_5^{2-}] \quad \text{(S5)}$$

$$RQSC = \frac{[SO_4^{\bullet-}]_{ss}}{\phi I_0 / V} \quad \text{(S6)}$$

$$= c_{PMS} b \frac{1-10^{-A}}{A} \left(\frac{10^{-pH}}{10^{-pKa_1}+10^{-pH}} \varepsilon_{HSO_5^-} + \frac{10^{-pKa_1}}{10^{-pKa_1}+10^{-pH}} \varepsilon_{SO_5^{2-}}\right)$$

$$\times \frac{k_{11}c_{BA} + k_{16}c_{TBA} + \frac{11}{6}\left(k_2 \frac{10^{-pH}}{10^{-pKa_1}+10^{-pH}} + k_3 \frac{10^{-pKa_1}}{10^{-pKa_1}+10^{-pH}}\right)c_{PMS}}{(k_{12}c_{BA} + k_{17}c_{TBA} + k_5 10^{pH-14})(k_{11}c_{BA} + k_{16}c_{TBA}) + (k_{12}c_{BA} + k_{17}c_{TBA} + \frac{1}{6}k_5 10^{pH-14})\left(k_2 \frac{10^{-pH}}{10^{-pKa_1}+10^{-pH}} + k_3 \frac{10^{-pKa_1}}{10^{-pKa_1}+10^{-pH}}\right)c_{PMS}}$$

Where $[SO_4^{\bullet-}]_{ss}$ is the quasi-stationary concentration of $SO_4^{\bullet-}$, A is the solution absorbance which was taken to be induced by PMS and BA (ε_{BA}= 760 $M^{-1}\cdot cm^{-1}$). It could be noted that the expression of *RQSC* as eq S6 might induce a bit error at pH ≥ 11, for the equilibrium constant of $HO^{\bullet}$ dissociation (pKa_2) is 11.9 (Table 1).

Text S4. The formation rates of $HO^{\bullet}$ and $SO_4^{\bullet-}$ in the UV/PMS system could be expressed as eqs S7 and S8, when NB and BA were used simultaneously as probe compounds in the UV/PMS system.

$$F_{HO^{\bullet}} = P_{PMS} + Q_{HO^{\bullet}} \quad \text{(S7)}$$

$$F_{SO_4^{\bullet-}} = P_{PMS} + T_{SO_4^{\bullet-}} - Q_{SO_4^{\bullet-}} \quad \text{(S8)}$$

$$Q_{HO^{\bullet}} = Q_{SO_4^{\bullet-}} \quad \text{(S9)}$$

where $F_{HO^{\bullet}}$ and $F_{SO_4^{\bullet-}}$ are the formation rates of $HO^{\bullet}$ and $SO_4^{\bullet-}$, P_{PMS} is the rate of PMS photolysis into $HO^{\bullet}$ or $SO_4^{\bullet-}$, $Q_{HO^{\bullet}}$ and $Q_{SO_4^{\bullet-}}$ are the production rate of $HO^{\bullet}$ and the consumption rate of $SO_4^{\bullet-}$ through the conversion of $SO_4^{\bullet-}$ to $HO^{\bullet}$, $T_{SO_4^{\bullet-}}$ is the production rate of $SO_4^{\bullet-}$ from the decay of $SO_5^{\bullet-}$.

The consumption rate of $HO^{\bullet}$ by probe compounds could be expressed as eq S10. The consumption rate of $SO_4^{\bullet-}$ by probe compounds could be expressed as eq S11, for the consumption rate of $SO_4^{\bullet-}$ by PMS was negligible compared with that caused by BA. Eqs S12 and S13 could be derived based on the kinetics of competitive reactions.

$$R_{HO^\bullet} = R_{HO^\bullet,NB} + R_{HO^\bullet,BA} + R_{HO^\bullet,PMS} \quad \text{(S10)}$$

$$R_{SO_4^{\bullet-}} = R_{SO_4^{\bullet-},BA} \quad \text{(S11)}$$

$$\frac{R_{HO^\bullet}}{R_{NB}} = \frac{R_{HO^\bullet}}{R_{HO^\bullet,NB}} = 1 + \frac{k_{11}c_{BA}}{k_{14}c_{NB}} + \frac{(\frac{10^{-pH}}{10^{-pKa_1}+10^{-pH}}k_2 + \frac{10^{-pKa_1}}{10^{-pKa_1}+10^{-pH}}k_3)c_{PMS}}{k_{14}c_{NB}} \quad \text{(S12)}$$

$$R_{SO_4^{\bullet-}} = R_{SO_4^{\bullet-},BA} = R_{BA} - R_{HO^\bullet,BA} = R_{BA} - \frac{k_{11}c_{BA}}{k_{14}c_{NB}}R_{NB} \quad \text{(S13)}$$

where $R_{HO^\bullet}$ is the consumption rate of $HO^\bullet$ by probe compounds, $R_{HO^\bullet,NB}$ is the consumption rate of $HO^\bullet$ by NB, $R_{HO^\bullet,BA}$ is the consumption rate of $HO^\bullet$ by BA, $R_{HO^\bullet,PMS}$ is the consumption rate of $HO^\bullet$ by PMS, $R_{SO_4^{\bullet-}}$ is the consumption rate of $SO_4^{\bullet-}$ by probe compounds, $R_{SO_4^{\bullet-},BA}$ is the consumption rate of $SO_4^{\bullet-}$ by BA, R_{BA} and R_{NB} are the consumption rates of BA and NB in the UV/PMS system, k_2, k_3, k_{11}, k_{14}, and pKa_1 are the rate constants shown in Table 1.

Based on the pseudo-steady state assumption of $SO_5^{\bullet-}$ and $k_{10a}/k_{10b} = 5$,[1] eq S14 could be derived.

$$T_{SO_4^{\bullet-}} = \frac{5}{6}R_{HO^\bullet,PMS} \quad \text{(S14)}$$

Hence, the formation rates of $HO^\bullet$ and $SO_4^{\bullet-}$ in the UV/PMS system could be expressed as eqs S15 - S17 and the rate of PMS photolysis into $HO^\bullet$ or $SO_4^{\bullet-}$ (P_{PMS}) could be derived as eq S18

$$F_{HO^\bullet} = R_{HO^\bullet} = R_{NB}(1 + \frac{k_{11}c_{BA}}{k_{14}c_{NB}} + \frac{(\frac{10^{-pH}}{10^{-pKa_1}+10^{-pH}}k_2 + \frac{10^{-pKa_1}}{10^{-pKa_1}+10^{-pH}}k_3)c_{PMS}}{k_{14}c_{NB}}) \quad \text{(S15)}$$

$$F_{SO_4^{\bullet-}} = R_{SO_4^{\bullet-}} = R_{BA} - \frac{k_{11}c_{BA}}{k_{14}c_{NB}}R_{NB} \quad \text{(S16)}$$

$$F_{total} = F_{HO^\bullet} + F_{SO_4^{\bullet-}} = R_{BA} + R_{NB} + \frac{(\frac{10^{-pH}}{10^{-pKa_1}+10^{-pH}}k_2 + \frac{10^{-pKa_1}}{10^{-pKa_1}+10^{-pH}}k_3)c_{PMS}}{k_{14}c_{NB}}R_{NB} \quad \text{(S17)}$$

$$P_{PMS} = \frac{1}{2}R_{BA} + \frac{1}{2}R_{NB} + \frac{1}{12}\frac{(\frac{10^{-pH}}{10^{-pKa_1}+10^{-pH}}k_2 + \frac{10^{-pKa_1}}{10^{-pKa_1}+10^{-pH}}k_3)c_{PMS}}{k_{14}c_{NB}}R_{NB} \quad \text{(S18)}$$

where F_{total} is the sum of the formation rates of $HO^\bullet$ and $SO_4^{\bullet-}$.

Text S5. ***Identification of radicals.*** TBA and methanol were used as radical scavengers for $HO^\bullet$ and both $HO^\bullet$ & $SO_4^{\bullet-}$, respectively (rate constants can be seen in Table 1). The degradation of BA in the UV/PMS system was obviously inhibited by the addition of TBA and methanol. The inhibition effect of methanol was more significant than TBA (Figure S3), which indicated that both $HO^\bullet$ and $SO_4^{\bullet-}$ contributed to BA degradation. This was also supported by the EPR results below, which indicated the existence of both $HO^\bullet$ and $SO_4^{\bullet-}$ in the UV/PMS system

DMPO was used as the spin trap in EPR measurements. No signal was observed in the absence of oxidant PMS or PDS (Figure S4a), which excluded the interruption induced by the photolysis of DMPO under given conditions. The EPR spectrum obtained from the photolysis of PMS was similar to that obtained from the photolysis of PDS (Figure S4b and c). The latter have already been proved to produce $SO_4^{\bullet-}$ by EPR spectra. The hyperfine coupling constants of DMPO radial adducts (obtained by simulation, a(N) 1.49 mT, a(H) 1.49 mT, all ± 0.05 mT) were consistent with the assignment of $HO^\bullet$ adduct. Additional species with hyperfine coupling constants of DMPO radial adducts (obtained by simulation, a(N) 1.38 mT, a(H) 1.02 mT, a(H) 0.14 mT, a(H) 0.08 mT, all ± 0.05 mT) were in accordance with the assignment of the $SO_4^{\bullet-}$

adduct.[2]

The DMPO $HO^{\bullet}$ adduct was reported to form by nucleophilic substitution of the DMPO $SO_4^{\bullet-}$ adduct via the reactions shown in Scheme S1.[3]

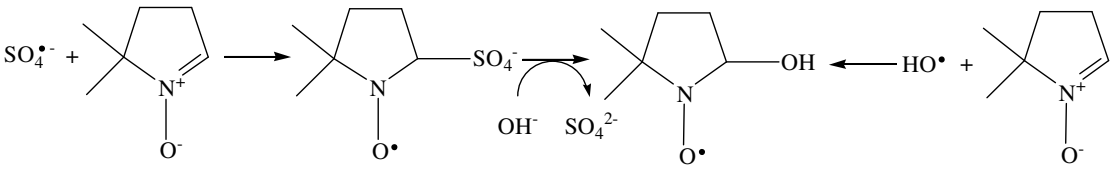

Scheme S1. Formation of DMPO adducts from $SO_4^{\bullet-}$ and $HO^{\bullet}$.

Since we could not kept the delay time consistent strictly before the measurement and the hydrolysis of DMPO $SO_4^{\bullet-}$ adduct to DMPO $HO^{\bullet}$ adduct was reported to be fast,[3] $HO^{\bullet}$ and $SO_4^{\bullet-}$ was just qualified but not quantified by measuring the intensity of EPR spectra of DMPO adducts under given experimental conditions. The signal for the OH-radicals appeared to be stronger during PDS photolysis than during PMS photolysis, which might be due to the delay in the measurement resulting in the hydrolysis of DMPO $SO_4^{\bullet-}$ adduct to DMPO $HO^{\bullet}$ adduct. Meanwhile, it could not be excluded that the higher initial pH for PDS photolysis might also contribute to the higher signal for the DMPO $HO^{\bullet}$ adduct.

Text S6. ***PMS decomposition.*** PMS was unstable and decomposed to H_2O_2 at basic pH.[2] The maximum rate of PMS spontaneous decomposition was found at the pH value equal to its second *p*Ka.[4] Hence, the experiments on PMS spontaneous decomposition were conducted at pH 9.4 (its second *p*Ka) and 11 (the pH value where the photolysis of PMS was the fastest observed subsequently). Catalase (from bovine

liver) with the concentration of 3.2 mg/L was used to quench H_2O_2 before measuring the concentration of PMS, and H_2O_2 would be completely consumed for a reaction time of 5 min if produced.[5] The spontaneous decomposition of PMS after 30min was less than 3% at either pH (data not shown), which indicated that the spontaneous decomposition of PMS to H_2O_2 was negligible over the studied pH range under given conditions.

Maruthamuthu and Neta[6] reported that $HO^{\bullet}$ could induce the acceleration of PMS decomposition and the rate constants of the reaction between $HO^{\bullet}$ and PMS were 1.7×10^7 $M^{-1}\cdot s^{-1}$ at pH 7 and 2.1×10^9 $M^{-1}\cdot s^{-1}$ at pH 11. The radical scavengers such as *tert*-butyl-alcohol (TBA), methanol, and BA were compared on reducing the decomposition of PMS from radical attack. Figure S6 shows that the decomposition of PMS in the UV/PMS system without the addition of radical scavengers was the fastest, followed by the case with the addition of BA, methanol and TBA in sequence. The stimulated effect of methanol on the decomposition of PMS as compared with TBA was similar to the results found in the UV/H_2O_2 system.[7] Hydroxylmethyl radical (α-hydroxyl-alkyl radical), formed from methanol by hydrogen abstraction, could reduce peroxides directly to form $HO^{\bullet}$ or $SO_4^{\bullet-}$. The carbon centered radical (β-hydroxyl-alkyl radical) from TBA by hydrogen abstraction was reported to be more stable than that from methanol and ethanol.[7] The above reasons might result in the different effects of TBA and methanol on PMS decomposition. Thus, the PMS decomposition in the UV/PMS system with the addition of TBA was used to indicate the photolysis of PMS.

Text S7. *The recalcitrance of NB to $SO_4^{\bullet-}$.* The rate constant of the reaction between NB and $SO_4^{\bullet-}$ was reported to be less than 10^6 $M^{-1}\cdot s^{-1}$.[8] In order to verify the recalcitrance of NB to $SO_4^{\bullet-}$, 20 mM TBA was used to compete for about 99% of $HO^{\bullet}$. Figure S7 shows that the degradation of NB was significantly inhibited when 20mM TBA was added. The degradation efficiency of NB in the UV/PMS system with the addition of TBA was almost the same as that achieved by UV alone, which indicated that $HO^{\bullet}$ should play an important role in NB degradation while $SO_4^{\bullet-}$ made little contribution to NB degradation.

Text S8. *The integration of the concentrations of $HO^{\bullet}$ and $SO_4^{\bullet-}$ ($IC_{HO^{\bullet}}$ and $IC_{SO_4^{\bullet-}}$).* In the UV/PMS system, when NB and BA were used simultaneously as the probe compounds, the kinetic expressions of BA and NB degradation could be expressed as follows:

$$-\frac{dc_{NB}}{dt} = k_{14}c_{NB}[HO^{\bullet}] \quad \text{(S19)}$$

$$-\frac{dc_{BA}}{dt} = k_{11}c_{BA}[HO^{\bullet}] + k_{12}c_{BA}[SO_4^{\bullet-}] \quad \text{(S20)}$$

$IC_{HO^{\bullet}}$ and $IC_{SO_4^{\bullet-}}$ could be expressed as eqs S21 and S22.

$$\int_0^t [HO^{\bullet}]dt = -\frac{1}{k_{14}}\int_{c_{0,NB}}^{c_{NB}} \frac{1}{c_{NB}} dc_{NB} \quad \text{(S21)}$$

$$\int_0^t [SO_4^{\bullet-}]dt = -\frac{1}{k_{12}}\left(\int_{c_{0,BA}}^{c_{BA}} \frac{1}{c_{BA}} dc_{BA} - \frac{k_{11}}{k_{14}}\int_{c_{0,NB}}^{c_{NB}} \frac{1}{c_{NB}} dc_{NB}\right) \quad \text{(S22)}$$

Though the complex calculation might enlarge the errors, it would exhibit the variations of the concentrations of $HO^{\bullet}$ and $SO_4^{\bullet-}$ in magnitude scale. $HO^{\bullet}$ dissociated into $O^{\bullet-}$ at pH >11, which made the calculation complicated. Therefore the calculation

of $IC_{HO^{\bullet}}$ and $IC_{SO_4^{\bullet-}}$ was performed at pH range from 7 to 11. $HO^{\bullet}$ was taken as its undissociated form over the studied pH range, which might introduce a little deviation from actual value at pH 11. Figure S10 shows that both $IC_{HO^{\bullet}}$ and $IC_{SO_4^{\bullet-}}$ increased with reaction time. The variations of $IC_{HO^{\bullet}}$ and $IC_{SO_4^{\bullet-}}$ with pH at given time were similar to the results shown in Figure 3a and b. $IC_{SO_4^{\bullet-}}$ was about one magnitude higher than $IC_{HO^{\bullet}}$ at pH ≤ 10. It could be due to the fast consumption of $HO^{\bullet}$ by BA and additional consumption by NB as compared with $SO_4^{\bullet-}$ in the UV/PMS system. The smaller difference between $IC_{HO^{\bullet}}$ and $IC_{SO_4^{\bullet-}}$ at pH 11 was due to the more consumption of $SO_4^{\bullet-}$ by HO^- to form $HO^{\bullet}$. It could be calculated from Figure S10 that the concentrations were in the magnitude of 10^{-13} - 10^{-12} M for $SO_4^{\bullet-}$ and 10^{-14} - 10^{-13} M for $HO^{\bullet}$, which indicated that the omission of the radical combination reactions in the UV/PMS system in the presence of BA was reasonable.

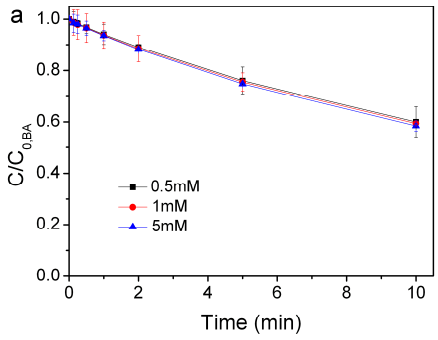

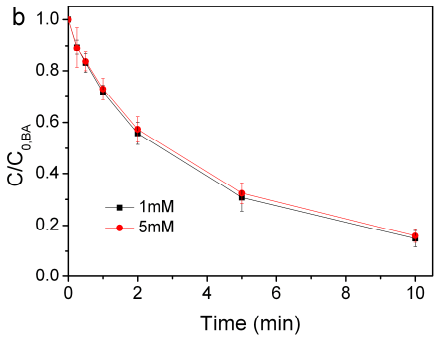

Figure S1. The influence of the concentration of phosphate buffer on BA degradation in the UV/PMS system at pH 7 (a) and pH 12 (b) (conditions: [PMS] = 100 μM as 1/2 Oxone; [BA] = 20.13 μM; Error bar represents a confidence interval with a confidence of 0.95).

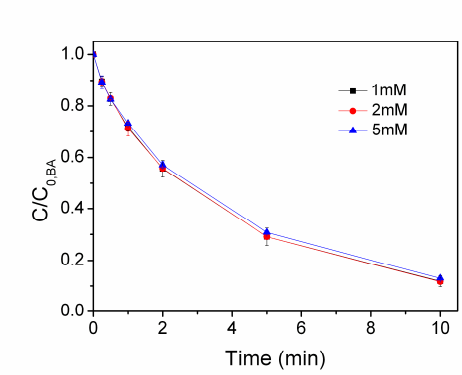

Figure S2. The influence of the concentration of borate buffer on BA degradation in the UV/PMS system (conditions: [PMS] = 100 μM as 1/2 Oxone; [BA] = 19.84 μM; pH = 10.0; Error bar represents a confidence interval with a confidence of 0.95).

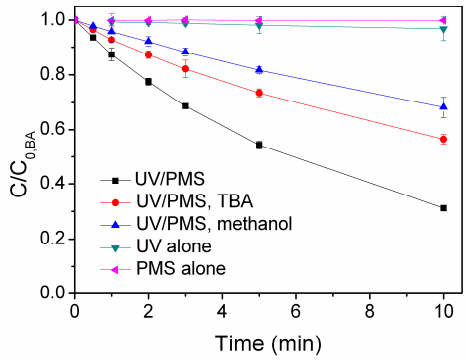

Figure S3. Oxidation of BA by PMS with or without UV irradiation (conditions: [BA] = 9.90 μM; [PMS] = 100 μM as 1/2 Oxone; [TBA] = 1 mM; [methanol] = 1 mM; pH = 7.0 ± 0.1; error bar represents a confidence interval with a confidence of 0.95).

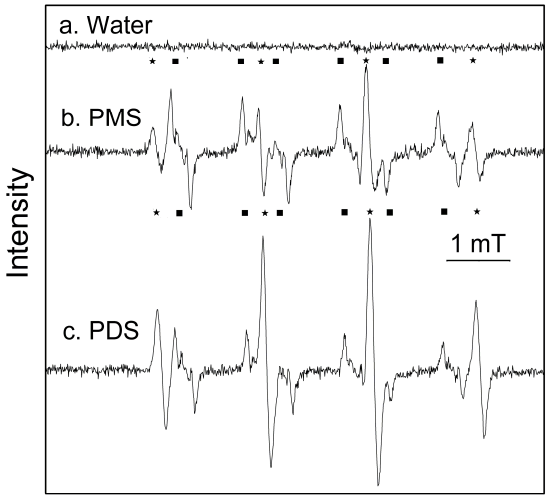

Figure S4. EPR spectra obtained from UV photolysis of PMS and PDS in the presence of DMPO (conditions: [PMS] = 0.04 M as 1/2 Oxone, pH = 2.2; [PDS] = 0.03 M, pH = 5.6; [DMPO] ≈ 0.15 N; ★ $HO^{\bullet}$ adduct; ■$SO_4^{\bullet-}$ adduct).

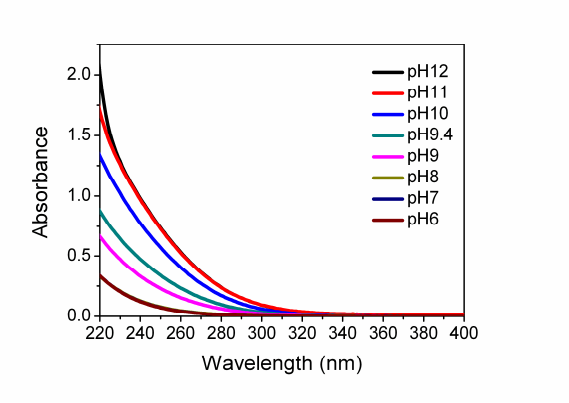

Figure S5. Absorption spectra of PMS solution at different pH (conditions: [PMS] = 4.25 mM)

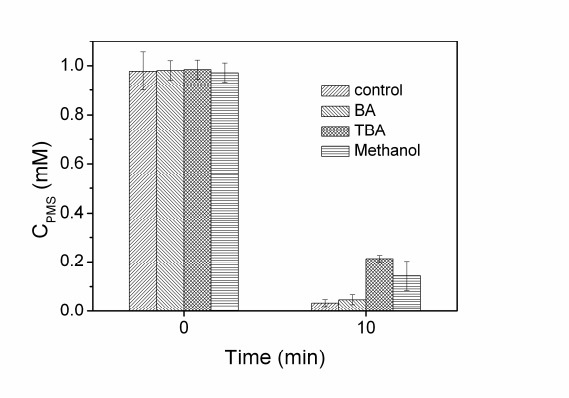

Figure S6. Decomposition of PMS in the UV/PMS system (conditions: [BA] = 9.90 μM; [TBA] = 100 mM; [methanol] = 100 mM; pH = 11.0; Error bar represents a confidence interval with a confidence of 0.95).

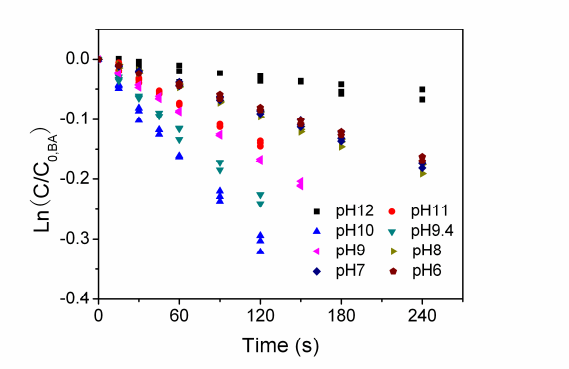

Figure S7. Kinetics of BA degradation in the UV/PMS system with the addition of TBA (conditions: [BA] = 9.90 μM; [PMS] = 100 μM as 1/2 Oxone; [TBA] = 10 mM).

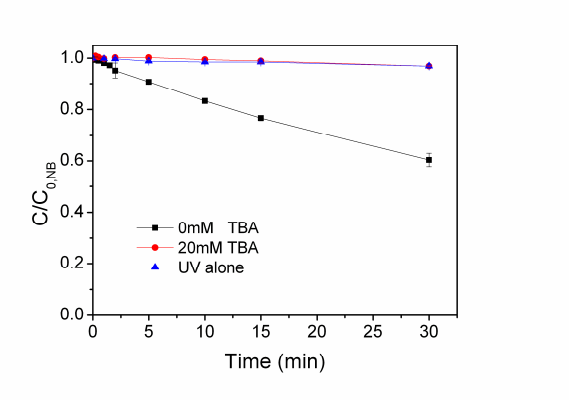

Figure S8. NB degradation in the UV/PMS system with or without the addition of TBA (conditions: [PMS] = 100 μM as 1/2 Oxone; [NB] = 18.07 μM; [TBA] = 20 mM; pH = 7.0; Error bar represents a confidence interval with a confidence of 0.95).

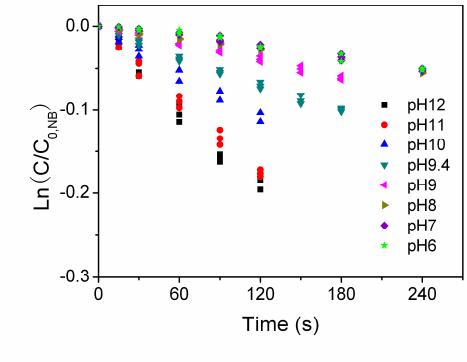

Figure S9. Kinetics of NB degradation in the UV/PMS system (conditions: [NB] = 18.07 μM; [BA] = 9.90 μM; [PMS] = 100 μM as 1/2 Oxone)

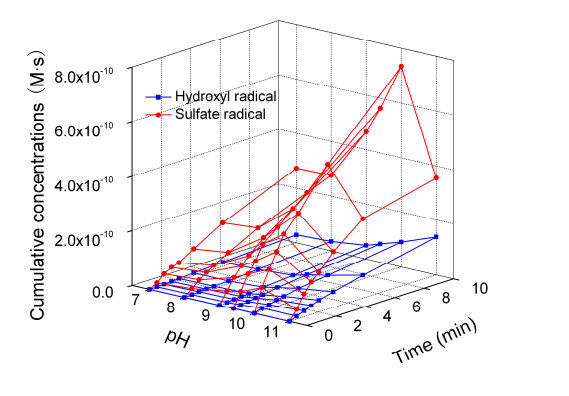

Figure S10. $IC_{HO^{\cdot}}$ and $IC_{SO_4^{\cdot-}}$ in the UV/PMS system (conditions: [NB] = 18.07 μM; [BA] = 9.90 μM; [PMS] = 100 μM as 1/2 Oxone).

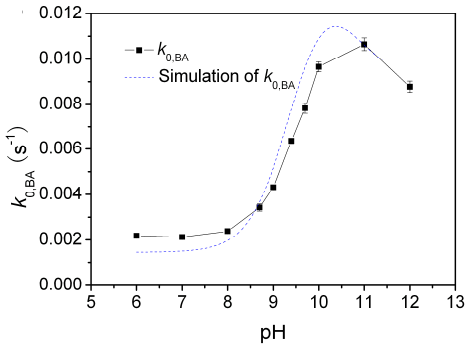

Figure S11. Simulation of $k_{0,BA}$ in the UV/PMS system at the pH range from 6 to 11 (conditions: [BA] = 9.90 μM; [PMS] = 100 μM as 1/2 Oxone).

Literature Cited:

(1) Yermakov, A. N.; Poskrebyshev, G. A.; Stoliarov, S. I. Temperature Dependence of the Branching Ratio of SO_5^- Radicals Self-Reaction in Aqueous Solution. *J. Phys. Chem.* **1996,** *100* (9), 3557-3560; DOI 10.1021/jp951330m.

(2) Furman, O. S.; Teel, A. L.; Watts, R. J. Mechanism of Base Activation of Persulfate. *Environ. Sci. Technol.* **2010,** *44* (16), 6423-6428; DOI 10.1021/es1013714.

(3) Timmins, G. S.; Liu, K. J.; Bechara, E. J. H.; Kotake, Y.; Swartz, H. M. Trapping of free radicals with direct in vivo EPR detection: A comparison of 5,5- dimethyl-1-

pyrroline - N - oxide and 5-diethoxyphosphoryl-5-methyl-1-pyrroline-N-oxide as spin traps for $HO^{\bullet}$ and $SO_4^{\bullet-}$. *Free Radic. Biol. Med.* **1999,** *27* (3-4), 329-333; DOI 10.1016/S0891-5849(99)00049-0.

(4) Ball, D. L.; Edwards, J. O. The kinetics and mechanism of the decomposition of caro's acid. *J. Am. Chem. Soc.,* **1956,** *78* (6), 1125-1129; DOI 10.1021/ja01587a011.

(5) Liu, W. J.; Andrews, S. A.; Stefan, M. I.; Bolton, J. R. Optimal methods for quenching H_2O_2 residuals prior to UFC testing. *Water Res.* **2003,** *37* (15), 3697-3703; DOI 10.1016/s0043-1354(03)00264-1.

(6) Maruthamuthu, P.; Neta, P. Radiolytic chain decomposition of peroxomonophosphoric and peroxomonosulfuric acids. *J. Phys. Chem.* **1977,** *81* (10), 937-940; DOI 10.1021/j100525a001.

(7) Popov, E.; Mametkuliyev, M.; Santoro, D.; Liberti, L.; Eloranta, J. Kinetics of UV-H_2O_2 advanced oxidation in the presence of alcohols: the role of carbon centered radicals. *Environ. Sci. Technol.* **2010,** *44* (20), 7827-7832; DOI 10.1021/es101959y.

(8) Neta, P.; Huie, R. E.; Ross, A. B. Rate constants for reactions of inorganic radicals in aqueous solution. *J. Phys. Chem. Ref. Data* **1988,** *17* (3), 1027-1284; Doi 10.1063/1.555808.